JOTCS A
Journal of the Turkish Chemical Society
Section: A
Chemistry
TURKISH CHEMICAL SOCIETY

Investigating the Effects of Fluorine Substituents on Organic Dyes in Dye-Sensitized Solar Cells

Saifaldeen Muwafag Abdalhadi[1*], Nabeel Mohammed[2], Khalida Ali Thejeel[3], Hazim Al-Zubaidi[4]

[1]Department of Remote Sensing, College of Remote Sensing and Geophysics, Al-Karkh University of Science, Baghdad, Iraq.
[2]Department of Biology, College of Education Al-Hawija, University of Kirkuk, Kirkuk, Iraq.
[3]Department of Geophysics, College of Remote Sensing and Geophysics, Al-Karkh University of Science, Baghdad, Iraq.
[4]Governmental programs department, Ministry of Higher Education and Scientific Research.

Abstract: We synthesized and evaluated five organic dyes that featured both mono- and di-substituted fluorine atoms for application in dye-sensitized solar cells (DSSCs). The dye structure was designed with *N, N*-dimethylaniline as a donor, fluorophenyl as an π-conjugated bridge, and cyanoacetic acid as an anchoring and acceptor group. The fluorine substituents are strong electron-withdrawing groups, introducing different numbers and positions of fluorine atoms (*ortho* and *meta*) that were expected to the ability of the acceptor parts of the dye. The results showed that adding the fluorine mono-substitution in the *ortho* position can enhance the efficiency of the solar cells in comparison with the meta-substitution and unsubstituted one. However, the di-substitution by fluorine atoms in two *ortho* positions and *ortho*, *meta* positions reduced the performance of the solar cells. The reason was related to the effect of π-conjugation between the fluorine substituent and the carbonyl group of the carboxylic acid. The DSSCs based on dye **14** achieved the best results with power conversion efficiency (PCE) = 3.33%, (J_{sc} = 5.43 mA cm^{-2}, V_{oc} = 0.81V and *FF* = 75.85%) under standard conditions with I_3^-/I^- as the electrolyte.

Keywords: Solar cells, DSSCs, organic dye, Suzuki cross-coupling reaction, and DFT.

Submitted: September 5, 2023. **Accepted:** October 16, 2023.

Cite this: Abdalhadi SM, Mohammed N, Thejeel KA, Al-Zubadi H. Investigating the Effects of Fluorine Substituents on Organic Dyes in Dye-Sensitized Solar Cells. JOTCSA. 2024;11(1):1-10.

DOI: http://doi.org/10.18596/jotcsa.1355244

***Corresponding author's E-mail:** dr.saifaldeen@kus.edu.iq

1. INTRODUCTION

Photovoltaic technologies have significantly developed over the last two decades, starting by investigating new types of solar cells such as quantum dot cells and thin film crystal cells, followed by improving the efficiency of other photovoltaic cells such as perovskite solar cells, from 14.0% to 22.1%, and three junction solar cells, from 32%.6 to 44.4% (1-5). In the present day, silicon solar cells are restricted to the photovoltaic market, despite their environmental effects and expensive production, the new generation of solar cells, such as dye-synthesized solar cells (DSSCs) has become one of the most important of the third generation solar cells due to their several advantages such as easy to fabrication, colorful, work in dark condition, vast design organic dye as an active layer and environmentally friendly (6-8). In addition, natural dyes could be used in DSSCs as an active layer, and carbonaceous material was used instead of expensive metals as an auxiliary electrode to reduce the cost of the fabrication process (9). The first report on DSSC was done by O'Regan and Grätzel in 1991 with an efficiency of 7.1% (10) and after several years, the efficiency of DSSC was improved to 14.7% (11).

The DSSCs were made from four main components: the first part is a photo-anode which is made from mesoporous nano-oxide layers such as TiO_2 or ZnO, the second part is a monolayer of organic or organometallic dye and was used as an active layer to harvest the light and generate the electrical power, the third part is the electrolyte solution and usually used iodine couple redox (I^-/I_3^-) in an aprotic

solvent to transfer the electron from auxiliary electrode to the dye. The last part is a counter electrode which is made from conductive glass coated by a platinum or graphene layer (12, 13).

The dyes of the DSSC play an important role in the efficiency of the solar cells and all the dyes should have photophysical and electrochemical properties such as luminescent, covering the ultraviolet-visible spectra to the near-infrared region, and hydrophobic properties to enhance the stability of the solar cells (14). Two types of dyes can be used as an active layer in DSSC; the first type is an organometallic dye, such as Ru-family complexes (N3, N719, and C101), (15-17) These have many advantages such as stability in the oxide state, gave instance charge transfer from metal to the ligand in the visible region and effective charge injection to the nano-semiconductor layer. The limitation of the organometallic dye is related to the cost of novel metal, low extinction coefficients, and decomposition or isomerization during purification (18, 19). The second type of dye is a metal-free organic dye and usually used dyes based on the chromophore such as coumarins (20), indolines (21), and triphenylamines (22) which absorb the light around 650 nm. These types of dyes usually have many advantages if compared with organometallic dyes such as high extinction coefficients (>2.50 × 10^4 M^{-1} cm^{-1}, in the visible region), flexibility in dye design, ease of purification and more economical than organometallic dye (23). In general, many efficient organic dyes have been reported with typical configuration for dye structure design, which is often considered as a donor π-bridge, and acceptor parts.

In this work, we designed and synthesized five simple organic free metal dyes with different fluorine positions and used these dyes as a dye in DSSCs (Scheme 1). The design of these dyes was represented by *N, N*-dimethylaniline as a donor part, benzene with different fluorine substitution as a π-conjugated bridge, and cyanoacetic acid as an acceptor part. All these dyes were characterized by ^{1}H NMR, ^{13}C NMR spectroscopies, and mass spectrometry, as well as all the results, were supported by the computational study. Several studies in the past were rented the fluorine atoms substitution in the π-bridge or acceptor parts in the organic dye for DSSCs and all of these introduced single position substitution within the molecular structure of the dye, (24, 25) thus improving the knowledge, we increased the substitution of the fluorine by mono-fluoro and di-fluoro at different positions. The idea for using fluorination to their spacer units was to create more efficient dyes for DSSCs by decreasing the lowest unoccupied molecular orbital (LUMO) energy level of the dye when increasing the number of fluorine atoms due to their highly electron-weighing ability as well as the fluorine atoms were substituted in π-bridge unit (benzene ring) for additional acceptor unit to improve the transfer of an electron from donor to anchoring group by electron-withdrawing effect and reduced the energy gap of the dye (26).

2. EXPERIMENTAL

2.1. General Information

All starting materials were supplied by Sigma-Aldrich® and Alfa Aesar®. The solvents were used without any purification. All reactions were performed under a nitrogen atmosphere and monitored using TLC plates. ^{1}H NMR spectra and ^{13}C NMR were recorded at 400 MHz and 100 MHz respectively on Bruker Avance III 400 spectrometers. UV-Vis absorption spectra were performed on a Shimadzu (UV-3600 UV-Vis-NIR spectrophotometer). The optical energy gap (E_{opt}) was calculated by using the absorption edge of the λ_{max} absorption peak by equation E_{opt} (eV) = 1240/λ (nm). Mass spectra were obtained on a JEOL SX-102A by using the fast atom bombardment (FAB) or electron impact (EI) technique. Elemental analysis was obtained on a Heraeus CHN-O Rapid Elementary Analyzer. The spectra are obtained in the Supplementary Information Section at the end of the article.

2.2. Synthesis

2.2.1. General procedure for the synthesis of compounds 7-11

Boronic acid derivative 1-5 (2.0 mmol) and 4-Bromo-*N, N*-dimethylaniline (0.40 g, 2.0 mmol) were introduced to the 2-neck round bottom flask under a nitrogen atmosphere. 1,4-dioxane (15 mL) was added and the reaction mixture was stirred for 10 min at 50 ℃. An aqueous solution of 2 M K_2CO_3 (0.20 mL, 0.40 mmol) and Pd(dppf)Cl_2 (6.3 mg) was added and the mixture was stirred at 100 ℃ (monitored by TLC). After 2 days, the mixture was cooled to room temperature, poured into cold water (40 mL), and extracted with dichloromethane (3 × 40 mL) in a separating funnel. The organic layer was dried over $MgSO_4$ and the solution was concentrated under reduced pressure. The crude compound was purified by column chromatography.

2.2.2. General procedure for the synthesis of compounds 13-17

Aldehyde derivative 7-11 (0.5 mmol), cyanoacetic acid (60 mg, 0.7 mmol), and $MgSO_4$ (60 mg, 0.26 mmol) were added in a mixture of acetonitrile and chloroform 1: 1 (10 mL + 10 mL), and the mixture was stirred for 15 minutes under nitrogen atmosphere. Piperidine (0.10 mL, 0.13 mmol) was added and the mixture was stirred at reflux for 6 hours. Afterward, the reaction was allowed to cool to room temperature, and cold water (50 mL) was added to the mixture in a separating funnel. The aqueous layer was extracted with ethyl acetate (3 × 40 mL) and then, the organic extracts were dried over $MgSO_4$. The crude solution was dried under vacuum and purified by column chromatography.

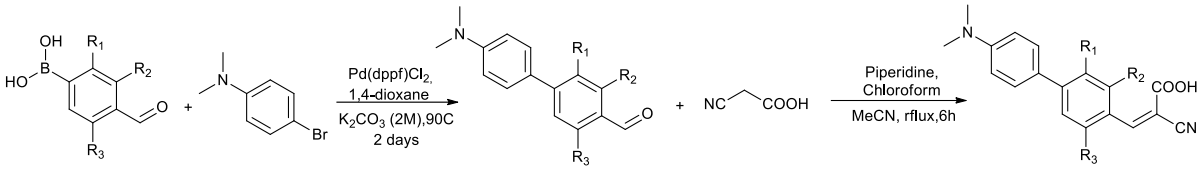

1 (R1=H, R2=H, R3=H)
2 (R1=H, R2=F, R3=H)
3 (R1=F, R2=H, R3=H)
4 (R1=F, R2=F, R3=H)
5 (R1=H, R2=F, R3=F)

6

7 (R1=H, R2=H, R3=H) (62%)
8 (R1=H, R2=F, R3=H) (71%)
9 (R1=F, R2=H, R3=H) (64%)
10 (R1=F, R2=F, R3=H) (59%)
11 (R1=H, R2=F, R3=F) (69%)

12

13 (R1=H, R2=H, R3=H) (78%)
14 (R1=H, R2=F, R3=H) (65%)
15 (R1=F, R2=H, R3=H) (75%)
16 (R1=F, R2=F, R3=H) (66%)
17 (R1=H, R2=F, R3=F) (62%)

Scheme 1: Synthesis of organic dyes **13**-**17** for DSSCs.

2.3. Spectral Data for the Products

4'-(dimethylamino)-[1,1'-biphenyl]-4-carbaldehyde (**7**) $C_{15}H_{15}NO$, m.p.:147-150 ℃; (^{1}H NMR, 400 MHz, DMSO, TMS) δ_H: 9.95 (s, 1H, CHO), 7.91 (d, 2H, J_{HH} = 7.8 Hz, CH-Ar), 7.73 (d, 2H, J_{HH}= 7.8 Hz. CH-Ar), 7.37 (d, 2H, J_{HH} = 6.8 Hz. CH-Ar), 6.88 (d, 2H, J_{HH} = 6.8 Hz. CH-Ar), 2.91 (s, 6H, NCH_3). (^{13}C NMR, 100 MHz, DMSO, TMS) δ_C: 191.90, 147.92, 143.52, 138.04, 131.23, 130.43, 128.14, 127.80, 114.58, 39.99. Anal. calcd.; C = 79.97; H = 6.71; N = 6.22. Found C,= 79.91; H = 6.75; N = 6.18. EI-MS: *m/z* 225.

4'-(dimethylamino)-3-fluoro-[1,1'-biphenyl]-4-carbaldehyde (**8**) $C_{15}H_{14}FNO$, m.p.:149-152 ℃; (^{1}H NMR, 400 MHz, DMSO, TMS) δ_H: 10.12 (s, 1H, CHO), 7.95 (d, 1H, J_{HH} = 10.5 Hz, CH-Ar), 7.60 (d, 2H, J_{HH} = 10.5 Hz,), 7.40 (d, 2H, J_{HH} = 8.1 Hz, CH-Ar), 6.87 (d, 2H, J_{HH} = 8.1 Hz, CH-Ar), 2.95 (s, 6H, NCH_3). (^{13}C NMR, 100 MHz, DMSO, TMS) δ_C: 185.79, 162.12, 148.44, 145.23, 138.82, 130.28, 128.62, 128.35, 124.29, 114.21, 113.68, 42.90. Anal. calcd.; C = 74.06; H = 5.80; N = 5.76; Found C = 73.98; H = 5.77; N = 5.69; EI-MS: *m/z* 243.

4'-(dimethylamino)-2-fluoro-[1,1'-biphenyl]-4-carbaldehyde (**9**) $C_{15}H_{14}FNO$, m.p.: 154-157 ℃; (^{1}H NMR, 400 MHz, DMSO, TMS) δ_H: 9.94 (s, 1H, CHO), 7.80 (m, 3H, CH-Ar), 7.75 (d, J_{HH}= 8.2 Hz, 2H, CH-Ar), 7.52 (d, J_{HH} = 8.2 Hz, 2H, CH-Ar), 2.98 (s, 6H, NCH_3). (^{13}C NMR, 100 MHz, DMSO, TMS) δ_C: 190.67, 158.67, 150.45, 139.09, 130.88, 128.77, 128.26, 127.90, 127.38, 115.79, 115.11, 44.61. Anal.calcd; C = 74.06; H = 5.80; N = 5.76; Found C = 74.71; H = 5.79; N = 5.77; EI-MS: *m/z* 243.

4'-(dimethylamino)-2,3-difluoro-[1,1'-biphenyl]-4-carbaldehyde(**10**) $C_{15}H_{13}F_2NO$, m.p. 166-169 ℃; (^{1}H NMR, 400 MHz, DMSO, TMS) δ_H: 10.14 (s, 1H, CHO), 7.71 (s, 1H, CH-Ar), 7.64 (s, 1H, CH-Ar), 7.58 (d, J_{HH} = 10.1 Hz, 2H, CH-Ar), 7.42 (d, J_{HH} = 10.1 Hz, 2H, CH-Ar), 2.99 (s, 6H, NCH_3). (^{13}C NMR, 100 MHz, DMSO, TMS) δ_C: 187.18, 149.59, 149.52, 145.20, 135.81, 128.83, 127.44, 126.35, 126.03, 123.45, 115.08, 43.22. Anal.calcd; C = 68.96; H = 5.02; N = 5.36; Found C = 69.05; H = 5.12; N = 5.33; EI-MS: *m/z* 261.

4'-(dimethylamino)-3,5-difluoro-[1,1'-biphenyl]-4-carbaldehyde(**11**) $C_{15}H_{13}F_2NO$, m.p. 164-167 ℃; (^{1}H NMR, 400 MHz, DMSO, TMS) δ_H: 10.15 (s, 1H, CHO), 7.55 (s, CH-Ar), 7.40 (d, J_{HH} = 9.3 Hz, 2H, CH-Ar), 6.97 (d, J_{HH} = 9.3 Hz, 2H, CH-Ar), 2.94 (s, 6H, NCH_3). (^{13}C NMR, 100 MHz, DMSO, TMS) δ_C: 180.68, 160.83, 148.63, 145.90, 130.16, 128.45, 114.16, 111.71, 110.04, 42.01. Anal.calcd; C = 68.96; H = 5.02; N = 5.36 Found C = 69.02; H = 5.02; N = 5.38; EI-MS: *m/z* 261.

(*E*)-2-cyano-3-(4'-(dimethylamino)-[1,1'-biphenyl]-4-yl)acrylic acid (**13**) $C_{18}H_{16}N_2O_2$, m.p. > 250 ℃; (^{1}H NMR, 400 MHz, DMSO, TMS) δ_H: 8.48 (s, 1H, C=CH), 7.51(d, J_{HH} = 7.1, 2H, CH-Ar), 7.49 – 7.41 (m, 4H, CH-Ar), 6.74 (d, J_{HH} = 7.8, 2H, CH-Ar), 2.88 (s, 6H, CH_3). (^{13}C NMR, 100 MHz, DMSO, TMS) δ_C: 162.67, 147.92, 140.14, 138.99, 133.97, 130.44, 128.82, 127.80, 114.57, 111.24, 102.51, 41.90. Anal.calcd; C = 73.95; H = 5.52; N = 9.58; Found C = 73.88; H = 5.49; N = 9.59; (FAB)$^+$ [M]$^+$: *m/z* 292.

(*E*)-2-cyano-3-(4'-(dimethylamino)-3-fluoro-[1,1'-biphenyl]-4-yl)acrylic acid (**14**) $C_{18}H_{15}FN_2O_2$, m.p. > 250 ℃; (^{1}H NMR, 400 MHz, DMSO, TMS) δ_H: 8.45 (s, 1H, C=CH), 7.54 – 7.40 (m, 5H, CH-Ar), 6.76 (d, J_{HH} = 7.1 Hz, 2H, CH-Ar), , 2.92 (s, 6H, CH-Ar). (^{13}C NMR, 100 MHz, DMSO, TMS) δ_C: 162.07, 159.15, 156.53, 148.44, 143.74, 141.18, 130.36, 129.81, 128.35, 126.34, 119.28, 114.89, 111.24, 105.75, 42.98. Anal.calcd; C = 69.67; H = 4.87; N = 9.03; Found C = 69.63; H = 4.91; N = 8.96; (FAB)$^+$ [M]$^+$: *m/z* 310.

(*E*)-2-cyano-3-(4'-(dimethylamino)-2-fluoro-[1,1'-biphenyl]-4-yl)acrylic acid (**15**) $C_{18}H_{15}FN_2O_2$, m.p. > 250 ℃; (^{1}H NMR, 400 MHz, DMSO,TMS) δ_H; 8.44 (s, 1H, C=CH), 7.60 (d, J_{HH} = 7.8 Hz, 1H, CH-Ar), 7.42 (d, J_{HH} = 10.2 Hz, 2H, CH-Ar), 7.29 (d, J_{HH} = 7.8 Hz, 2H, CH-Ar) 6.76 (d, J_{HH} = 10.2 Hz, 2H, CH-Ar), 2.81 (s, 6H, CH_3). (^{13}C NMR, 100 MHz, DMSO, TMS) δ_C; 161.97, 159.35, 150.45, 139.10, 133.58, 128.79, 126.76, 126.49, 124.48, 115.11, 113.17, 111.24, 102.58, 42.01. Anal.calcd; C = 69.67; H = 4.87; N = 9.03; Found C = 69.60; H = 4.77; N = 9.12; (FAB)$^+$ [M]$^+$: *m/z* 310.

(*E*)-2-cyano-3-(4'-(dimethylamino)-2,3-difluoro-[1,1'-biphenyl]-4-yl)acrylic acid (**16**) $C_{18}H_{14}F_2N_2O_2$, m.p. > 250 ℃; (^{1}H NMR, 400 MHz, DMSO, TMS) δ_H: 8.49 (s, 1H, C=CH), 7.44 (d, 2H, J_{HH} = 6.4 Hz, CH-Ar),7.34 (s, 1H, CH-Ar), 7.22 (s, 1H, CH-Ar), 6.75 (d, J_{HH} = 6.4 Hz, 2H, CH-Ar), 2.80 (s, 6H, CH_3). (^{13}C NMR, 100 MHz, DMSO,TMS) δ_C: 162.87, 149.59, 146.99, 145.09, 142.46, 129.71, 128.83, 127.43, 126.35, 122.66, 121.90, 115.08, 109.25, 104.69, 43.09. Anal.calcd; C = 65.85; H = 4.30; N = 8.53; Found C = 65.71; H = 4.31; N = 8.59; (FAB)$^+$ [M]$^+$: *m/z* 328.

(*E*)-2-cyano-3-(4'-(dimethylamino)-3,5-difluoro-[1,1'-biphenyl]-4-yl)acrylic acid (**17**) $C_{18}H_{14}F_2N_2O_2$, m.p. > 250 ℃; (^{1}H NMR, 400 MHz, DMSO, TMS) δ_H: 8.51 (s, 1H, C=CH), 7.49 (d, 2H, J_{HH} = 9.0 Hz, CH-Ar), 7.27 (s, 2H, CH-Ar), 6.84 (d, J_{HH} = 9.0 Hz, 2H, CH-Ar), 2.81 (s, 6H, CH_3). (^{13}C NMR, 100 MHz, DMSO, TMS) δ_C; 163.01, 160.59, 157.96, 148.63,145.84, 142.32, 130.16, 128.54, 114.16, 112.21, 111.24, 111.19, 108.77, 43.17. Anal.calcd; C, 65.85; H, 4.30; N, 8.53; Found C, 65.82; H, 4.33; N, 8.48; $(FAB)^+$ $[M]^+$: *m/z* 328.

3. FABRICATION OF DSSCs

Indium tin oxide (ITO) glass sheets (2 cm × 2 cm, 15 Ω/sq) were cleaned in distilled water by using an ultrasonic bath (5 minutes) and then rinsed with absolute ethanol. The TiO_2 paste was prepared by adding absolute ethanol (5 mL) to the TiO_2 nano-powder (3 g, ~ 25 nm) with grinding for 15 minutes, then added acetic acid (0.1 mL) and Triton X-100 (0.05 mL) to paste with grinding for 30 minutes to prevent the aggregation of the TiO_2 particles .

The doctor blade technique was used to prepare the TiO_2 film on ITO glass by applying two parallel strips of scotch tape on the conductive side of the ITO glass to deposit the TiO_2 past on the conductive glass between the two pieces of the scotch tape and coating by the doctor blade method. After one hour the scotch tape was removed carefully and the coated glass was dried for 15 minutes at 75 °C and then sintered for 45 minutes at 400 °C, Finally, the coated glass was cooled down to room temperature, and then placing the coated glass to the solution of the dye for 2 hours under dark condition. The electrolyte solution I_3^-/I^- was formed by adding 1.0 M KI and 0.10 M I_2 to the acetonitrile solvent and stored in a dark container. H_3PtCl_6 solution in isopropanol (3 mg/mL) was used to prepare the counter electrode of the cells by depositing the solution onto ITO glass by spin coating technique. Finally, coated glass and counter electrode were combined with added few drops of electrolyte solution on an active layer for the photovoltaic measurement device.

4. RESULT AND DISCUSSION

4.1. Synthesis

Five dyes with different fluoro substitutions (**13**-**17**) were prepared according to Scheme 1. These dyes were synthesized by using two simple steps involving the Suzuki cross-coupling reaction the and Knoevenagel condensation reaction. The first step was represented by a Suzuki cross-coupling reaction between 4-Bromo-*N*, *N*- dimethylaniline, and boronic acid derivatives (**1**-**5**) by using $Pd(dppf)Cl_2$ as a catalyst and this reaction gave a good yield (~ 60%-70%). The next step was obtained with a Knoevenagel condensation reaction to prepare the final compound (**13**-**17**). The reaction was performed between aldehyde derivatives (**7**-**11**) and cyanoacetic acid with a small amount of piperidine as a catalyst and the yields of final products were rounded between ~ 62%-78%. There is a big difference between the yields of the final compounds and that is because of the steric hindrance between fluorine atoms and the cyanoacetic acid group which led to a decrease in the quantity of the yield.

4.2. Optical properties

The UV-Vis spectra of five compounds are shown in Figure 1 and the related photochemical properties are reported in Table 1. All organic compounds show two significant absorption peaks at 280-320 nm and 440-500 nm. The first absorption peaks are attributed to the electron transition of π - π*, and the second absorption bands are attributed to the transition of intramolecular charge transfer (ICT) from a donor (dimethylaniline) to an acceptor (cyanoacetic acid). It is not much different in the absorption maxima between these dyes. However, the absorption maxima band of compounds **15** and **16** exhibited a slight red shift from the original compound **13**, while the compounds **14** and **17** showed a blue shift and that could be from the steric effect between fluorine atoms in ortho position and cyanoacetic acid part as well as deportation of a carboxylic acid with the solvent (27, 28). The range of molar extinction coefficients of these compounds is between 2.22-2.30 × 10^4 M^{-1} cm^{-1} and that is higher than from standard dye N719 (1.41 × 10^4 M^{-1} cm^{-1}) which is given a good light harvesting nature for the dyes.

Table 1: Shows the optical and theoretical parameters of the dyes (**13**-**17**).

Compound	λ_{abs}[a](nm)	λ_{max}[b] (ε × 10^{-4}, dm^3 mol^{-1} cm^{-1})	E_{opt}[c] (eV)	E_{HOMO}[d] (eV)	E_{LUMO}[d] (eV)	E_{gap}[d]
13	474	2.26	2.07	-5.71	-3.09	2.48
14	458	2.28	2.23	-5.58	-3.17	2.41
15	502	2.22	1.96	-5.65	-3.28	2.42
16	489	2.25	2.10	-5.62	-3.28	2.34
17	467	2.27	2.09	-5.51	-3.29	2.22

[a] Maximum of absorption in THF (1 × 10^{-4} M), [b] extinction coefficient, [c] optical energy gap, and [d] theoretical calculation.

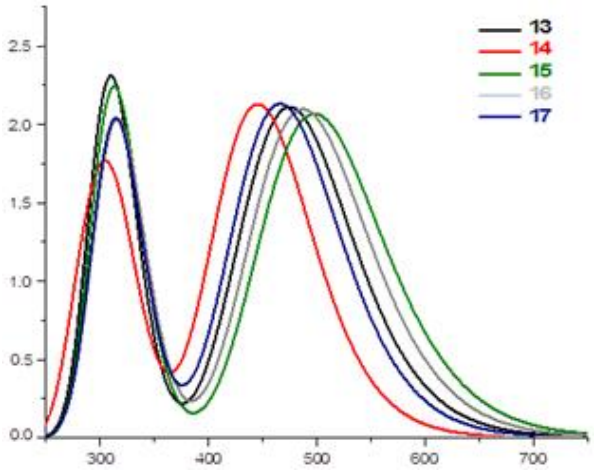

Figure 1: Absorption spectra of dyes **13-17** in THF (1×10^{-4}). Y axis is absorbance, and X axis is wavelength in nanometers.

4.3. Theoretical Calculations

Density functional theory (DFT) and time-dependent-density functional theory (TD-DFT) were calculated using Gaussian 09. The geometry optimization of all dyes and the vibrational harmonic frequencies were computed using Becke's three-parameter hybrid, and Lee Yang Parr's gradient corrected correlation (B3LYP) functional with standard split valence 6-311G (d,p) as a basis set under vacuum (29). All the calculations have been done by using the polarization function for heavy atoms (d) and hydrogen atoms (p). All results show the absence of imaginary frequency which indicates that the optimizations of all structures were rare energy minima (30). The optimization geometry (Figure 2) of the dyes was observed as the dihedral angle between two benzene rings of about 30̊, for compounds **13**, **14,** and **17**, while this angle was evaluated to 35̊ for compounds **15** and **16** due to the steric effect between fluorine atom and the other benzene ring. These angles gave good solubility for all the dyes because they prevent aggregation due to π-stacks between the surfaces of molecules (31).

The highest occupied molecular orbital (HOMO) and lowest unoccupied molecular orbital (LUMO) were reported in Figure 2 and Table 1. For all dyes, the electron distribution of HOMO was delocalized in the donor part (dimethylaniline) and the electron distribution of LUMO was spread over the acceptor's arm (Fluoro- benzene and cyanoacetic acid) which is indicative that gave a good charge separation during the excitation process. The HOMOs level of the dyes **13**,**14**,**15**,**16**, and **17** are -5.7, -5.58, -5.65, -5.62, and 5.51 eV, respectively and all of these levels are lower than the energy level of the electrolyte solution I_3^-/I^- (-4.8) which indicate that the excited electron was relaxed easily form energy level of redox solution to the HOMOs level of the dyes. Also, the LUMOs level of the dyes **13**,**14**,**15**,**16**, and **17** are -3.09, -3.17, -3.28, -3.28, and -3.29 respectively and all of these levels are higher than the conduction band (CB) of the TiO_2 (-4.0 eV) which indicate that the excited electron was easily transfer from HOMOs level of the dyes to the CB of the TiO_2 (32).

The lowest energy gap was represented with compound **17,** (2.22 eV) due to the effect of two fluorine atoms with high electronegativity, which decreased the LUMO level of the dye, while the highest energy gap was illustrated with compound **13**, (2.48 eV) which indicate that the π-bridge with the fluorine atom played the important role in the excitation of electrons. The energy gap of the dyes is arranged in order **13** (2.48 eV), **15** (2.42 eV), **14** (2.41 eV), **16** (2.34 eV), **17** (2.22 eV).

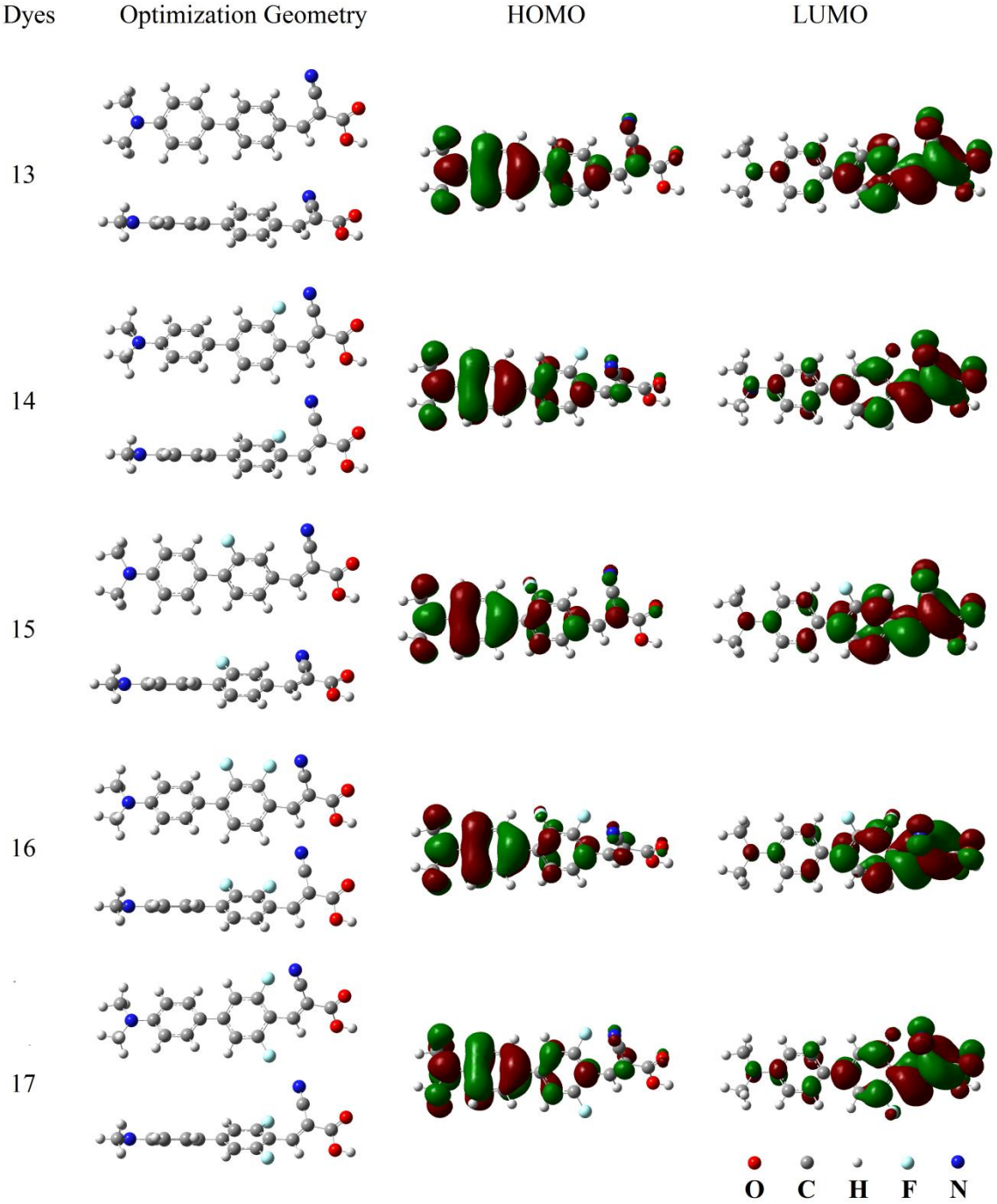

Figure 2: The optimization geometries, HOMOs, and LUMOs for prepared dyes.

4.5 Device Testing and Photovoltaic Performance

The photovoltaic properties were investigated for all dyes in DSSCs, the current density and voltaic performance (*J-V*) were measured in Table 2 and shown in Figure 3. The measurements of the solar cells were done under the standard condition at AM 1.5G and solar irradiation (100 mW cm^{-2}). The control dye N719 was included as a comparison. In general, the performances of dyes **13**, **14**, and **15** were slightly better than difluoro substitution and that could be due to the deviation conformation (steric effect) between the bulk cyanoacrylate group and difluorophenyl moieties, which decreased the effect of π-conjugation. The dye **14** exhibited a higher power conversion efficiency (PCE) of 3.33% with a J_{sc} of 5.43 mA cm^{-2}, V_{oc} of 0.81 V, and *FF* of 75.85%. While compound **16** showed a lower PCE of 2.14% under the same condition (J_{sc} = 3.94 mA cm^{-2}, V_{oc} of 0.80 V, and *FF* of 71.10%). The DSSCs devices based on compound **14** exhibited a higher J_{sc} and molar extinction coefficient, which compensated for the negative impact of the UV-Vis absorption spectra. Furthermore, compared with dye **13** (non-fluorine substitution), dye **14** and **15** (mono-fluorine substitution) gives slightly higher current density 5.43 and 5.08 mA cm^{-2} respectively, while compound **16** and **17** (di-fluoro substitution) shows slightly lower current density 3.94 and 4.14 mA cm^{-2} respectively, which indicate that the compound **14** and **15** had a strong electronic coupling with the surface (TiO_2) and hence increase of the dye uptake. On the other hand, the efficiency of the dyes was affected directly by the fluorine atom position, the *ortho*-fluorine substituted **14** gives a higher PCE than *meta*-fluorine substituted **15** and that could be by

the resonance conjugation between the *ortho*-fluorine substituted and carbonyl group of carboxylic acid which increased the basicity of dye and improvement the TiO_2 affinity.

Table 2: Photovoltaic performance of the DSSCs under global conditions (AM 1.5, 100 mW cm^{-2}).

Dye	J_{sc} (mA cm^{-2})	V_{oc} (V)	*FF* (%)	PCE (%)
13	4.52	0.87	76.68	3.01
14	5.43	0.81	75.85	3.33
15	5.08	0.80	76.63	3.11
16	3.94	0.80	71.10	2.41
17	4.14	0.82	74.90	2.54
N719	10.30	0.92	79.96	7.57

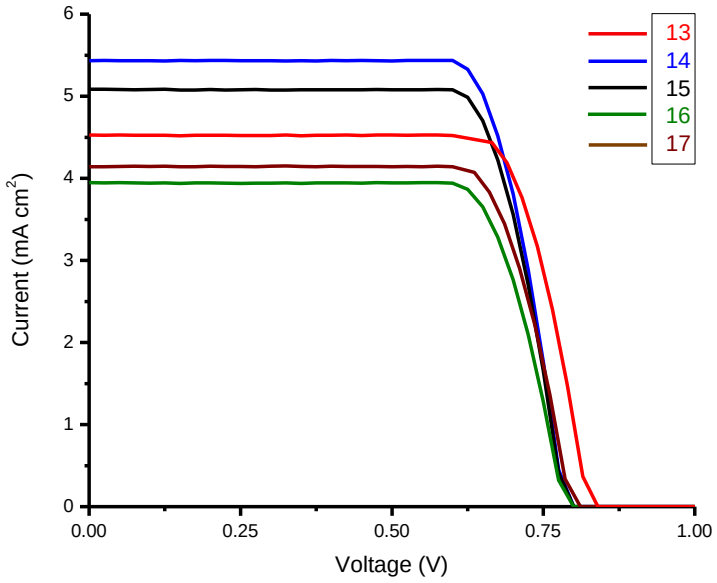

Figure 3: Current density vs. voltage (*J*–*V*) curves for dyes **13**,**14**,**15**,**16**, and **17**.

5. CONCLUSION

In summary, a series of non-metal dyes containing different fluoro-positions on a π-bridge were analyzed. The mono-fluoro substituted compounds exhibited similar PCE values to the non-substituted ones. In contrast, the di-fluoro substituted showed a lower PCE due to increasing the dihedral angle between the benzene ring and the cyanoacetic acid group and that reduced the ability of the conjugation system, therefore the value of J_{sc} was low. The device based on dyes **14** and **15** had higher J_{sc} values (5.48 and 5.08 mA cm^{-2} respectively) than dyes **13**, **16**, and **17** (4.52, 3.94, and 4.14 mA cm^{-2} respectively) which was in agreement with PCE values of the dyes. These results showed that the addition of electron-withdrawing on the ortho position could increase the PCE of the DSSCs.

6. CONFLICT OF INTEREST

There are no conflicts of interest.

7. ACKNOWLEDGMENT

The researchers acknowledged Al-Karkh University of Science for support and funding.

8. REFERENCES

1. Sharma S, Jain KK, Sharma A. Solar Cells: In Research and Applications—A Review. Mater Sci Appl [Internet]. 2015 Dec 1;06(12):1145–55. Available from: <URL>.

2. Abdulrazzaq OA, Saini V, Bourdo S, Dervishi E, Biris AS. Organic Solar Cells: A Review of Materials, Limitations, and Possibilities for Improvement. Part Sci Technol [Internet]. 2013 Sep 3;31(5):427–42. Available from: <URL>.

3. Ajayan J, Nirmal D, Mohankumar P, Saravanan M, Jagadesh M, Arivazhagan L. A review of photovoltaic performance of organic/inorganic solar cells for future renewable and sustainable energy technologies. Superlattices Microstruct [Internet]. 2020 Jul 1;143:106549. Available from: <URL>.

4. Day J, Senthilarasu S, Mallick TK. Improving spectral modification for applications in solar cells: A review. Renew Energy [Internet]. 2019 Mar 1 [cited 2023 Oct 24];132:186–205. Available from: <URL>.

5. Abdulhussein SF, Abdalhadi SM, Hanoon HD. Synthesis of new imidazole derivatives dyes and application in dye sensitized solar cells supported by

DFT. Egypt J Chem [Internet]. 2022 Feb 5;65(9):211–7. Available from: <URL>.

6. Abdalhadi SM, Al-Baitai AY, Al-Zubaidi HA. Synthesis and Characterization of 2,3-Diaminomaleonitrile Derivatives by One-Pot Schiff Base Reaction and Their Application in Dye Synthesized Solar Cells. Indones J Chem [Internet]. 2020 Dec 22;21(2):443. Available from: <URL>.

7. Cariello M, Abdalhadi SM, Yadav P, Decoppet J-D, Zakeeruddin SM, Grätzel M, et al. An investigation of the roles furan *versus* thiophene π-bridges play in donor–π-acceptor porphyrin based DSSCs. Dalt Trans [Internet]. 2018;47(18):6549–56. Available from: <URL>.

8. Abdalhadi SM, Connell A, Zhang X, Wiles AA, Davies ML, Holliman PJ, et al. Convenient synthesis of EDOT-based dyes by CH-activation and their application as dyes in dye-sensitized solar cells. J Mater Chem A [Internet]. 2016;4(40):15655–61. Available from: <URL>.

9. Gong J, Sumathy K, Qiao Q, Zhou Z. Review on dye-sensitized solar cells (DSSCs): Advanced techniques and research trends. Renew Sustain Energy Rev [Internet]. 2017 Feb;68:234–46. Available from: <URL>.

10. O'Regan B, Grätzel M. A low-cost, high-efficiency solar cell based on dye-sensitized colloidal TiO_2 films. Nature [Internet]. 1991 Oct;353(6346):737–40. Available from: <URL>.

11. Kakiage K, Aoyama Y, Yano T, Oya K, Fujisawa J, Hanaya M. Highly-efficient dye-sensitized solar cells with collaborative sensitization by silyl-anchor and carboxy-anchor dyes. Chem Commun [Internet]. 2015;51(88):15894–7. Available from: <URL>.

12. Devadiga D, Selvakumar M, Shetty P, Santosh MS. Dye-Sensitized Solar Cell for Indoor Applications: A Mini-Review. J Electron Mater [Internet]. 2021 Jun 1;50(6):3187–206. Available from: <URL>.

13. Mohammed N, Shakkor SJ, Abdalhadi SM, Al-Bayati YK. Two multifunctional benzoquinone derivatives as small molecule organic semiconductors for bulk heterojunction and perovskite solar cells. Main Gr Chem [Internet]. 2022 Dec 20;21(4):943–52. Available from: <URL>.

14. Sharma K, Sharma V, Sharma SS. Dye-Sensitized Solar Cells: Fundamentals and Current Status. Nanoscale Res Lett [Internet]. 2018 Dec 28;13(1):381. Available from: <URL>.

15. Talodthaisong C, Wongkhan K, Sudyoadsuk T, Saengsuwan S, Jitchati R. Comparison of the DSSC Efficiency on Synthetic N3 Dyes. Adv Mater Res [Internet]. 2015 Dec;1131:165–8. Available from: <URL>.

16. Portillo-Cortez K, Martínez A, Dutt A, Santana G. N719 Derivatives for Application in a Dye-Sensitized Solar Cell (DSSC): A Theoretical Study. J Phys Chem A [Internet]. 2019 Dec 26;123(51):10930–9. Available from: <URL>.

17. Liu S, Liu J, Wang T, Wang C, Ge Z, Liu J, et al. Preparation and photovoltaic properties of dye-sensitized solar cells based on zinc titanium mixed metal oxides. Colloids Surfaces A Physicochem Eng Asp [Internet]. 2019 May;568:59–65. Available from: <URL>.

18. Numata Y, Islam A, Chen H, Han L. Aggregation-free branch-type organic dye with a twisted molecular architecture for dye-sensitized solar cells. Energy Environ Sci [Internet]. 2012;5(9):8548–52. Available from: <URL>.

19. Ahmad S, Guillén E, Kavan L, Grätzel M, Nazeeruddin MK. Metal free sensitizer and catalyst for dye sensitized solar cells. Energy Environ Sci [Internet]. 2013;6(12):3439–66. Available from: <URL>.

20. Sarrato J, Pinto AL, Malta G, Röck EG, Pina J, Lima JC, et al. New 3-Ethynylaryl Coumarin-Based Dyes for DSSC Applications: Synthesis, Spectroscopic Properties, and Theoretical Calculations. Molecules [Internet]. 2021 May 14;26(10):2934. Available from: <URL>.

21. Al-horaibi SA, Asiri AM, El-Shishtawy RM, Gaikwad ST, Rajbhoj AS. Indoline and benzothiazole-based squaraine dye-sensitized solar cells containing bis-pendent sulfonate groups: Synthesis, characterization and solar cell performance. J Mol Struct [Internet]. 2019 Nov;1195:591–7. Available from: <URL>.

22. Pati PB, Yang W, Zade SS. New dyes for DSSC containing triphenylamine based extended donor: Synthesis, photophysical properties and device performance. Spectrochim Acta Part A Mol Biomol Spectrosc [Internet]. 2017 May;178:106–13. Available from: <URL>.

23. Lee C-P, Lin RY-Y, Lin L-Y, Li C-T, Chu T-C, Sun S-S, et al. Recent progress in organic sensitizers for dye-sensitized solar cells. RSC Adv [Internet]. 2015;5(30):23810–25. Available from: <URL>.

24. Chang YJ, Chow TJ. Highly efficient triarylene conjugated dyes for sensitized solar cells. J Mater Chem [Internet]. 2011;21(26):9523–31. Available from: <URL>.

25. Chen D-Y, Hsu Y-Y, Hsu H-C, Chen B-S, Lee Y-T, Fu H, et al. Organic dyes with remarkably high absorptivity; all solid-state dye sensitized solar cell and role of fluorine substitution. Chem Commun [Internet]. 2010;46(29):5256–8. Available from: <URL>.

26. Chen B-S, Chen D-Y, Chen C-L, Hsu C-W, Hsu H-C, Wu K-L, et al. Donor–acceptor dyes with fluorine substituted phenylene spacer for dye-sensitized solar cells. J Mater Chem [Internet]. 2011;21(6):1937–45. Available from: <URL>.

27. Wang Z-S, Cui Y, Dan-oh Y, Kasada C, Shinpo A, Hara K. Thiophene-Functionalized Coumarin Dye for Efficient Dye-Sensitized Solar Cells: Electron

Lifetime Improved by Coadsorption of Deoxycholic Acid. J Phys Chem C [Internet]. 2007 May 1;111(19):7224–30. Available from: <URL>.

28. Yang H-Y, Yen Y-S, Hsu Y-C, Chou H-H, Lin JT. Organic Dyes Incorporating the Dithieno[3,2-*b*:2′,3′- *d*]thiophene Moiety for Efficient Dye-Sensitized Solar Cells. Org Lett [Internet]. 2010 Jan 1;12(1):16–9. Available from: <URL>.

29. Frisch MJ, Trucks GW, Schlegel HB, Scuseria GE, Robb MA, Cheeseman JR, et al. Gaussian 16 Rev. C. 01, Wallingford, CT. Wallingford, CT. 2016;

30. Chen X, Jia C, Wan Z, Yao X. Organic dyes with imidazole derivatives as auxiliary donors for dye-sensitized solar cells: Experimental and theoretical investigation. Dye Pigment [Internet]. 2014 May;104:48–56. Available from: <URL>.

31. Aulakh RK, Sandhu S, Tanvi, Kumar S, Mahajan A, Bedi RK, et al. Designing and synthesis of imidazole based hole transporting material for solid state dye sensitized solar cells. Synth Met [Internet]. 2015 Jul;205:92–7. Available from: <URL>.

32. Duvva N, Eom YK, Reddy G, Schanze KS, Giribabu L. Bulky Phenanthroimidazole–Phenothiazine D−π–A Based Organic Sensitizers for Application in Efficient Dye-Sensitized Solar Cells. ACS Appl Energy Mater [Internet]. 2020 Jul 27;3(7):6758–67. Available from: <URL>.